A Dynamic Graph-Based Scheduling and Interference Coordination Approach in Heterogeneous Cellular Networks

Li Zhou, Xiping Hu, Edith C.-H. Ngai, *Member, IEEE*, Haitao Zhao, *Member, IEEE*, Shan Wang, Jibo Wei, and Victor C. M. Leung, *Fellow, IEEE*

***Abstract*—To meet the demand of increasing mobile data traffic and provide better user experience, heterogeneous cellular networks (HCNs) have become a promising solution to improve both the system capacity and coverage. However, due to dense self-deployment of small cells in a limited area, serious interference from nearby base stations may occur, which results in severe performance degradation. To mitigate downlink interference and utilize spectrum resources more efficiently, we present a novel graph-based resource allocation and interference management approach in this paper. First, we divide small cells into cell clusters, considering their neighborhood relationships in the scenario. Then, we develop another graph clustering scheme to group user equipment (UE) in each cell cluster into UE clusters with minimum intracluster interference. Finally, we utilize a proportional fairness scheduling scheme to assign subchannels to each UE cluster and allocate power using water-filling method. To show the efficacy and effectiveness of our proposed approach, we propose a dual-based approach to search for optimal solutions as the baseline for comparisons. Furthermore, we compare the graph-based approach with the state of the art and a distributed approach without interference coordination. The simulation results show that our graph-based approach reaches more than 90% of the optimal performance and achieves a significant improvement in spectral efficiency compared with the state of the art and the distributed approach both under cochannel and orthogonal deployments. Moreover, the proposed graph-based approach has low computation complexity, making it feasible for real-time implementation.**

***Index Terms*—Cluster, graph based, heterogeneous networks, resource allocation, small cell.**

Manuscript received December 25, 2014; revised April 7, 2015; accepted May 14, 2015. Date of publication May 20, 2015; date of current version May 12, 2016. This work was supported in part by the National Natural Science Foundation of China under Grant 61002032 and Grant 91338105; by the 863 Project under Grant 2014AA01A701; and by the Foundation of Science and Technology on Information Transmission and Dissemination in the Communication Networks Laboratory, National Key Laboratory of Anti-Jamming Communication Technology. The review of this paper was coordinated by Prof. W. Song.

L. Zhou, H. Zhao, S. Wang, and J. Wei are with College of Electronic science and Engineering, National University of Defense Technology, Changsha 410073, China (e-mail: zhouli2035@nudt.edu.cn; haitaozhao@nudt.edu.cn; chinafir@nudt.edu.cn; wjbhw@nudt.edu.cn).

X. Hu and V. C. M. Leung are with the Department of Electrical and Computer Engineering, The University of British Columbia, Vancouver, BC V6T 1Z4, Canada (e-mail: xipingh@ece.ubc.ca; vleung@ece.ubc.ca).

E. C.-H. Ngai is with the Department of Information Technology, Uppsala University, SE-751 05 Uppsala, Sweden (e-mail: edith.ngai@it.uu.se).

Color versions of one or more of the figures in this paper are available online at http://ieeexplore.ieee.org.

Digital Object Identifier 10.1109/TVT.2015.2435746

I. Introduction

With the ever-increasing demand of wireless services and exponential increase in mobile data traffic driven by widely used wireless smart devices (smartphones, tablets, laptops, etc.), future cellular networks face a great challenge to meet this overwhelming demand of network capacity. The Global Mobile Data Traffic Forecast Report provided by Cisco predicts that the global mobile data traffic will reach 15.9 EB (1 EB $= 10^{18}$ B) per month or a run rate of 190 EB annually by 2018 [1]. A small-cell or heterogeneous cellular network (HCN) is considered one of the most promising technologies for enhancing coverage and capacity of wireless networks. However, the widespread deployment of small cells inevitably brings severe interference among user equipment (UE). Due to the unplanned and dynamic feature of small cells, interference coordination among them is much more challenging than that in traditional macrocell networks. Long-Term Evolution (LTE) and the following standards have developed a wide range of physical-layer techniques such as backhaul-based signaling and beamforming to mitigate interference [2]. However, this research direction is still in its infancy. There is still a huge space for improvement in the context of resource allocation and scheduling.

Resource allocation in orthogonal frequency-division multiplexing (OFDM)-based wireless networks have been extensively studied as OFDM has become the core technology of contemporary wireless networks. In OFDM-based networks, subchannels and power are the two main resources that need to be reasonably assigned to improve the system performance. In LTE HCNs, base stations are denoted by e-NodeBs (eNBs). In the downlink scenario, subchannels and power are assigned by the eNBs taking the channel state information (CSI) and quality of service (QoS) requirements into account.

The joint allocation of subchannel and power is considered an NP-hard problem in OFDM-based wireless networks [3]. In this paper, we propose a novel graph-based approach combining cell clustering and UE clustering to mitigate interference and allocate resources in small-cell networks. Cell clustering and UE clustering are considered two graph-partitioning manipulations. To begin with, we aggregate small cells into cell clusters based on their neighboring relations. We further develop a UE clustering scheme to group UEs in each cell cluster into UE clusters with minimum intracluster interference. Then, we

adopt a proportional fair subchannel allocation method that assigns subchannels to the UE clusters of each cell cluster. Finally, we apply water-filling method [4] in each cell to optimize power in their assigned subchannels. We evaluate this method in both cochannel and orthogonal deployments. In cochannel deployments, macro and small cells operate on the same frequency band, whereas in orthogonal deployments, the spectrum is divided into two parts, with one part allocated to the macrocells and the other to the small cells. Cochannel deployments are often utilized when the spectrum is limited, whereas orthogonal deployments mitigate interference at the cost of available spectrum resource. In cochannel deployments, the closer a small-cell eNB (SeNB) to a macrocell eNB (MeNB), the smaller coverage it has due to interference. On the contrary, in orthogonal deployments, the coverage of small cells is not affected by the MeNBs.

The major contributions of this paper are summarized as follows.

1) We propose a novel graph-based approach combining cell clustering and UE clustering to mitigate interference and allocate resources in small-cell networks. The proposed graph-based approach has low complexity and near-optimal performance, which is feasible for real-time implementation.
2) We introduce a graph-partitioning scheme called cell clustering, which adopts the homogeneous Poisson point process model of SeNBs to decide their downlink coverage and aggregates small cells into cell clusters based on their neighboring relations. This manipulation can reduce the complexity of the problem significantly, particularly in dense small-cell network scenarios.
3) We define weighted graphs to represent the interference relationships of UEs and develop another graph-partitioning scheme named UE clustering, which divides the UEs in the same cell cluster into UE clusters with minimum intracluster interference.
4) We present a dual-based approach to obtain the optimal solution, which provides a baseline to evaluate the graph-based approach.
5) We evaluate the performance of the proposed graph-based approach with extensive simulations and compare it with the state of art and two baseline approaches, which are the dual-based approach and the distributed approach without interference coordination. The results show that the graph-based approach can achieve an outstanding tradeoff between performance and efficiency.

The remainder of this paper is organized as follows. We briefly summarize the existing work in Section II. Section III gives an overview of the system model and formulates our defined problem. Section IV proposes our graph-based approach in three steps. In Section V, we introduce a dual-based approach to search for the optimal solution of the problem. To show the efficacy and effectiveness of our proposed approach, we provide simulation results in Section VI. Finally, Section VII concludes this paper.

II. Related Work

There are two kinds of interference existing in LTE HCNs, i.e., cotier interference and cross-tier interference [5]. In a two-tier HCN, cotier interference occurs between small cells when they have overlapping coverage, whereas cross-tier interference occurs between a macrocell and a small cell when the SeNB is in the coverage of the macrocell. Resource allocation considering interference coordination is a hot topic in LTE networks and has been widely studied [6]–[8]. These approaches are generally based on adaptive subband scheduling and time-domain resource partitioning. There are several heuristics to resolve this problem in the existing literature [9]–[12], which resort to intelligent algorithms or game theory. Unfortunately, these methods usually require a relatively long time to converge to a solution, so that it is hard to support real-time applications.

Recently, graph-based methods have attracted the attention of researchers considering their low computational complexity and good performance [13]. In this context, a typical graph is the interference graph representing the interference relationships among vertices. In [14], two categories of interference graphs are introduced. One is called the conflict graph [15], where the edges denote critical interference. Two vertices of such a graph can only have a connecting edge when one imposes interference on the other and *vice versa*. The second type of graph is the weighted graph [16]. The weight of an edge in such a graph represents the interference strength between its two connecting vertices.

In general, vertices represent eNBs or UEs. For the graphs that take eNBs as vertices, a common method to mitigate interference is to aggregate eNBs into clusters and assign different subchannels to different clusters [13], [17]. The edges represent the potential cochannel interference between eNBs, and graph coloring is often used for cluster segmentation. The problem of this method is that further partitioning on the subchannels may lead to inefficient spectrum usage. More importantly, since the spectrum resources are allocated in the unit of subchannel or resource block in downlink LTE systems, fewer UEs would be served if the number of subchannels available for an eNB is reduced. The problem is even worse in small-cell networks due to their highly dynamic nature. For the graphs that consider UEs as vertices in small-cell networks, we can only find limited work from the existing literature. The difficulty lies in two aspects. The first one is the definition of the metric for the potential interference relationships among UEs. The second is dealing with the large scale of the problem. As we know, there are usually many more UEs than eNBs in the network. In particular, when the deployment of small cells becomes dense, placing all UEs in the graph results in squared increment in the number of edges as we consider the interference relationship between each UE pair. Consequently, we need to find an efficient way to reduce the scale of the graph.

In our previous work [18], we proposed a simple graph-based approach that considers the typical coverage of small cells and the relative channel gain of UEs as the metric. Based on the previous work, we propose an improved graph-based approach including cell clustering and UE clustering in this paper. Cell clustering is designed according to the distribution

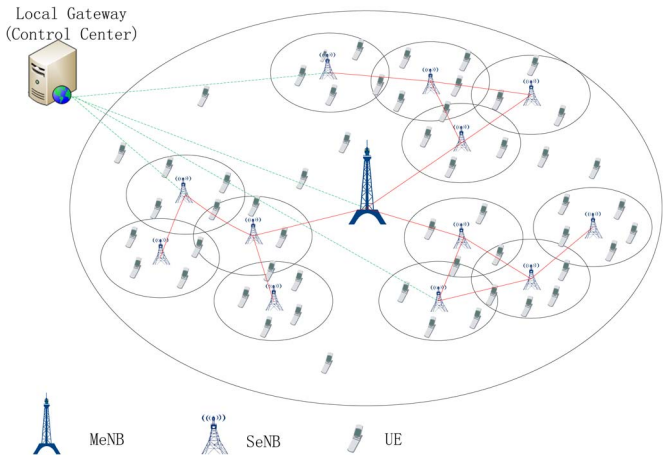

Fig. 1. Typical two-tier HCN.

of downlink signal-to-interference-plus-noise ratio (SINR) of eNBs to reduce the scale of the problem by splitting the original graph of eNBs into cell clusters. UE clustering is conducted using a new metric named relative interference in each cell cluster. Finally, subchannels are assigned among UE clusters in each cell cluster, and transmit power is allocated in each cell.

III. System Model and Problem Formulation

Here, we introduce the system model and present the problem formulations for cochannel and orthogonal deployments.

A. System Model

In this paper, we consider a two-tier HCN that consists of a macrocell and several small cells. Fig. 1 shows a typical network. The set of small cells is represented by the set $\mathbf{S} = \{1, 2, \ldots, S\}$. To model a real scenario, the small cells are arbitrarily distributed inside the network. The MeNB and all SeNBs are connected to a local gateway, which works as a centralized controller and manages the scheduling and resource allocation task in the network [19]. The physical channels between eNBs and UEs are modeled by frequency-selective Rayleigh fading on top of distance-based attenuation. At the beginning of each time slot, a training process is conducted for the centralized controller or eNBs to obtain global CSI. Research on efficient channel training and estimation methods has been reported in [20] and [21]. Training and estimation are performed at the eNBs to obtain the channel gains from them to the UEs. Finally, all these acquired channel gains are notified to the centralized controller. Channel estimation or channel prediction has been studied extensively in the past several years in the context of OFDM [22], [23]. These studies have been shown to improve the robustness of the system and reduce the amount of feedback overhead. We assume ideal channel condition in this paper. The notations used in the system model are summarized in Table I.

For notational simplicity, we use subscripts "m" and "s" to distinguish the attributes of the parameters, where "m" implies that the parameter is associated with the macrocell, whereas "s" indicates that the parameter is used for small cells. We assume that there are M_m UEs in the macrocell and $M_{s,i}$ UEs in small cell i, where $M_s = \sum_{i\in\mathbf{S}} M_{s,i}$, and $M = M_m + M_s$. We define $\mathbf{M}_m$ and $\mathbf{M}_{s,i}(i \in \mathbf{S})$, respectively, as the set of UEs in the macrocell, i.e., macrocell UEs (MUEs), and the sets of UEs in the small cells, i.e., small-cell UEs (SUEs). The total spectrum is divided into N subchannels, and the set of the subchannels is given by $\mathbf{N} = \{1, 2, \ldots, N\}$. In cochannel deployments, all subchannels are shared by the two tiers, while in orthogonal deployments, we assume that there are N_m subchannels assigned to macrocell and $N_s = N - N_m$ subchannels assigned to small cells. $\mathbf{N}_m$ and $\mathbf{N}_s$ are the sets of subchannels assigned to the macrocell and small cells, respectively. For simplicity, we assume that the MeNB and SeNBs are equipped with omnidirectional antennas and their maximum transmit power levels are denoted by P_m and $P_{s,i}(i \in \mathbf{S})$, respectively. Furthermore, we assume that the coverage areas of the eNBs are determined by their downlink SINR distribution. The coverage areas of cells in cochannel deployments and orthogonal deployments can be quite different because of cross-tier interference in cochannel deployments, i.e., the MeNB and SeNBs interfere with each other. On the other hand, in orthogonal deployments, there is no cross-tier interference.

In cochannel deployments, if the MeNB transmits data to MUE k through subchannel n, the MUE receives interference from SeNBs. As a result, the SINR at the MUE can be expressed as $\gamma_{m,k,n} = p_{m,k,n}g_{m,k,n}/(\sum_{i\in\mathbf{S}}\sum_{q\in\mathbf{M}_{s,i}} p_{s,i,q,n}g_{s,i,k,n} + \delta^2)$, where $p_{m,k,n}$ is the allocated power for MUE k on subchannel n by the MeNB, $g_{m,k,n}$ is the channel gain from the MeNB to MUE k on subchannel n, $p_{s,i,q,n}$ is the allocated power for SUE q on subchannel n by SeNB i, $g_{s,i,k,n}$ is the channel gain between SeNB i and MUE k on subchannel n, and δ^2 is the power of thermal noise per subchannel. Similarly, for SUEs, if SeNB i transmits data to SUE k through subchannel n, the corresponding SINR at the SUE is $\gamma_{s,i,k,n} = p_{s,i,k,n}g_{s,i,k,n}/(\sum_{q\in\mathbf{M}_m} p_{m,q,n}g_{m,k,n} + \sum_{j\in\mathbf{S},j\neq i}\sum_{q\in\mathbf{M}_{s,j}} p_{s,j,q,n}g_{s,j,k,n} + \delta^2)$.

In orthogonal deployments, the SINR at MUE k from the MeNB and SUE k from SeNB i are, respectively, $\gamma_{m,k,n} = p_{m,k,n}g_{m,k,n}/\delta^2$ and $\gamma_{s,i,k,n} = p_{s,i,k,n}g_{s,i,k,n}/(\sum_{j\in\mathbf{S},j\neq i}\sum_{q\in\mathbf{M}_{s,i}} p_{s,j,q,n}g_{s,j,k,n} + \delta^2)$.

The Shannon capacity that can be achieved by MUE k from the MeNB and SUE k from SeNB i are represented by $R_{m,k,n} = \log_2(1+\Gamma\cdot\gamma_{m,k,n})$ and $R_{s,i,k,n} = \log_2(1+\Gamma\cdot\gamma_{s,i,k,n})$, respectively, where Γ indicates the SINR gap under a given bit error rate (BER) and is defined as $\Gamma = -1.5/\ln(\text{BER})$ [24].

The optimization problem explained herein is to find the optimal resource (subchannel and power) allocations that maximize the overall network capacity. Let $w_{m,k}$ and $w_{s,i,k}$ be the weights that are assigned, respectively, to MUE k and SUE k based on fairness considerations. Binary variable $x_{m,k,n}$ indicates if subchannel n has been assigned $(x_{m,k,n} = 1)$ or not assigned $(x_{m,k,n} = 0)$ to MUE k. Similarly, $x_{s,i,k,n}$ is the indication variable of the subchannel assignment for SUE k in small cell i.

B. Problem Formulation for Cochannel Deployments

Based on the given definitions, the problem in cochannel deployments can be formulated as a capacity maximization

TABLE I
NOTATION SUMMARY OF SYSTEM MODEL

Notation	Description
$\mathbf{S}$; S	Set of active small cells in the network; number of small cells
$\mathbf{M}_m$; M_m	Set of MUEs; number of MUEs
$\mathbf{M}_{s,i}$; $M_{s,i}$	Set of SUEs in small cell i; number of SUEs in small cell i
$\mathbf{N}$; N	Set of all subchannels; total number of subchannels
$\mathbf{N}_m$; N_m	Set of subchannels for the macrocell; number of subchannels for the macrocell
$\mathbf{N}_s$; N_s	Set of subchannels for small cells; number of subchannels for small cells
$p_{m,k,n}$	Allocated power on subchannel n for UE k by the MeNB
$p_{s,i,k,n}$	Allocated power on subchannel n for UE k by SeNB i
$x_{m,k,n}$	Indicator on subchannel n for UE k by the MeNB
$x_{s,i,k,n}$	Indicator on subchannel n for UE k by SeNB i
$g_{m,k,n}$	Gain of subchannel n between the MeNB and UE k
$g_{s,i,k,n}$	Gain of subchannel n between SeNB i and UE k in small cell i
$R_{m,k,n}$	Capacity of subchannel n between the MeNB and MUE k
$R_{s,i,k,n}$	Capacity of subchannel n between SeNB i and SUE k in small cell i
$w_{m,k}$	Weight assigned to MUE k
$w_{s,i,k}$	Weight assigned to SUE k in small cell i
P_m; $P_{s,i}$	Maximum transmit power of MeNB and SeNB i
$\gamma_{m,k,n}$	SINR of UE k receives from the MeNB on subchannel n
$\gamma_{s,i,k,n}$	SINR of UE k receives from SeNB i on subchannel n
Γ	SINR gap
BER	Bit error rate
δ^2	Thermal noise power per subchannel

problem as follows:

$$\begin{aligned}
\max\ & \sum_{k\in\mathbf{M}_m} w_{m,k} \sum_{n\in\mathbf{N}} x_{m,k,n} R_{m,k,n} \\
& + \sum_{i\in\mathbf{S}} \sum_{k\in\mathbf{M}_{s,i}} w_{s,i,k} \sum_{n\in\mathbf{N}} x_{s,i,k,n} R_{s,i,k,n} \\
\text{s.t.}\ & \text{C1}: x_{m,k,n} \in \{0,1\} \qquad \forall k \in \mathbf{M}_m, n \in \mathbf{N} \\
& \text{C2}: x_{s,i,k,n} \in \{0,1\} \qquad \forall i \in \mathbf{S}, k \in \mathbf{M}_{s,i}, n \in \mathbf{N} \\
& \text{C3}: p_{m,k,n} \geq 0 \qquad \forall k \in \mathbf{M}_m, n \in \mathbf{N} \\
& \text{C4}: p_{s,i,k,n} \geq 0 \qquad \forall i \in \mathbf{S}, k \in \mathbf{M}_{s,i}, n \in \mathbf{N} \\
& \text{C5}: \sum_{k\in\mathbf{M}_m} x_{m,k,n} \leq 1 \\
& \text{C6}: \sum_{k\in\mathbf{M}_{s,i}} x_{s,i,k,n} \leq 1 \qquad \forall i \in \mathbf{S} \\
& \text{C7}: \sum_{k\in\mathbf{M}_m} \sum_{n\in\mathbf{N}} p_{m,k,n} \leq P_m \\
& \text{C8}: \sum_{k\in\mathbf{M}_{s,i}} \sum_{n\in\mathbf{N}} p_{s,i,k,n} \leq P_{s,i} \qquad \forall i \in \mathbf{S} \qquad (1)
\end{aligned}$$

where the objective represents the weighted summation of the total capacity of the system. C1, C2, C5, and C6 are the Boolean constraints for subchannel assignments, which indicate that a subchannel can be assigned to one UE at most. C3, C4, C7, and C8 are the linear constraints for power allocations, including individual power and total power constraints.

C. Problem Formulation for Orthogonal Deployments

In orthogonal deployments, the macrocell and small cells can be treated independently because they do not interfere with each other. For the macrocell, we can utilize the traditional single-cell resource allocation scheme [25], whereas for small cells, the problem can be presented as

$$\begin{aligned}
\max\ & \sum_{i\in\mathbf{S}} \sum_{k\in\mathbf{M}_{s,i}} w_{s,i,k} \sum_{n\in\mathbf{N}_s} x_{s,i,k,n} R_{s,i,k,n} \\
\text{s.t.}\ & \text{C9}: x_{s,i,k,n} \in \{0,1\} \qquad \forall i \in \mathbf{S}, k \in \mathbf{M}_{s,i}, n \in \mathbf{N}_s \\
& \text{C10}: p_{s,i,k,n} \geq 0 \qquad \forall i \in \mathbf{S}, k \in \mathbf{M}_{s,i}, n \in \mathbf{N}_s \\
& \text{C11}: \sum_{k\in\mathbf{M}_{s,i}} x_{s,i,k,n} \leq 1 \qquad \forall i \in \mathbf{S} \\
& \text{C12}: \sum_{k\in\mathbf{M}_{s,i}} \sum_{n\in\mathbf{N}_s} p_{s,i,k,n} \leq P_{s,i} \qquad \forall i \in \mathbf{S} \qquad (2)
\end{aligned}$$

where the objective expresses the weighted summation of the capacity of all small cells. C9 and C11 are the Boolean constraints for subchannel assignments. C10 and C12 are the linear constraints for power allocations.

The optimization problems (1) and (2) are mixed-integer programming problems, which have been proven to be NP-hard [3]. Therefore, searching global optimal solutions in the whole solution space typically involves exponential computational complexity. To solve the problems in a feasible way, we propose a low-complexity graph-based approach in Section IV and a dual-based approach in Section V.

IV. PROPOSED GRAPH-BASED APPROACH

Here, we introduce the graph-based downlink interference coordination and resource allocation approach, which assigns subchannels and power among UEs in the system that has been described earlier. The proposed graph-based approach includes three steps, which are 1) cell clustering, 2) UE clustering, and 3) subchannel and power allocation. Cell clustering aims

to aggregate small cells into cell clusters. UE clustering is designed to group UEs in each cell cluster into UE clusters with minimum intracluster interference. Subchannel allocation is conducted among UE clusters in each cell cluster, and power allocation is carried out in each cell.

A. Cell Clustering

The small cells that are closer to each other impose higher interference on the UEs inside. A simple idea is using these relations to deal with these cells together instead of handling individual small cell independently. We do not tackle them all together since the scale of the graph for UE clustering will be extremely large when the deployment of small cells is very dense. We first check all small cells in the network to determine whether there is neighboring relation between any two cells. Based on the neighboring relations, we construct the first type graph, in which vertices represent the S SeNBs. The edges describe the neighboring relations among the SeNBs. Two vertices are connected if they are neighbors. Second, we divide the graph into several cell clusters based on their neighboring relations. Although cell clusters are constructed from closer small cells, we take the interference from far away small cells into account while calculating interference.

The neighboring relationships are decided based on the SINR distribution of the eNBs. We model the SeNBs with a homogeneous Poisson point process [26] and denote the SINR by $\widehat{\gamma}$. In cochannel deployments, we define the SINR at a typical UE as

$$\widehat{\gamma}_m(x,y) = \frac{P_m \mathrm{Loss}_m(x,y)}{\sum_{i\in\mathbf{S}} P_{s,i}\mathrm{Loss}_{s,i}(x,y) + N\delta^2} \tag{3}$$

where (x,y) is the coordinate of the UE, $\mathrm{Loss}_m(x,y)$ is the path loss between the MeNB and the UE, and $\mathrm{Loss}_{s,i}(x,y)$ is the path loss between SeNB i and the UE.

The received SINR of SeNB i at (x,y) is

$$\widehat{\gamma}_{s,i}(x,y) = \frac{P_{s,i}\mathrm{Loss}_{s,i}(x,y)}{P_m\mathrm{Loss}_m(x,y) + \widehat{I}_{s,i}(x,y) + N\delta^2} \tag{4}$$

where $\widehat{I}_{s,i}(x,y) = \sum_{j\in\mathbf{S},j\neq i} P_{s,j}\mathrm{Loss}_{s,j}(x,y)$.

In orthogonal deployments, $\widehat{\gamma}_m(x,y)$ and $\widehat{\gamma}_{s,i}(x,y)$ are given by

$$\widehat{\gamma}_m(x,y) = \frac{P_m\mathrm{Loss}_m(x,y)}{N_m\delta^2} \tag{5}$$

$$\widehat{\gamma}_{s,i}(x,y) = \frac{P_{s,i}\mathrm{Loss}_{s,i}(x,y)}{\sum_{j\in\mathbf{S},j\neq i} P_{s,j}\mathrm{Loss}_{s,j}(x,y) + N_s\delta^2}. \tag{6}$$

The vertical profiles of the distributions of SINR for any two SeNBs are shown in Fig. 2. We define the minimum received SINR as Λ_{th}. When the received SINR at UE k from SeNB i is smaller than Λ_{th}, we assume that communication outage occurs or the UE is not in the coverage of SeNB i. We find that there always exists a balance location at the connecting line of any two SeNBs, where a UE receives the same SINR from the two SeNBs. This point is shown as the intersection of the respective SINR curves. We assume that the coordinate of the balance location is (x^*,y^*); thus, we have $\widehat{\gamma}_{s,i}(x^*,y^*) = \widehat{\gamma}_{s,j}(x^*,y^*)$. If the coverage areas of two small cells overlap or the SINR at the balance location exceeds Λ_{th}, we claim that the two SeNBs are neighbors.

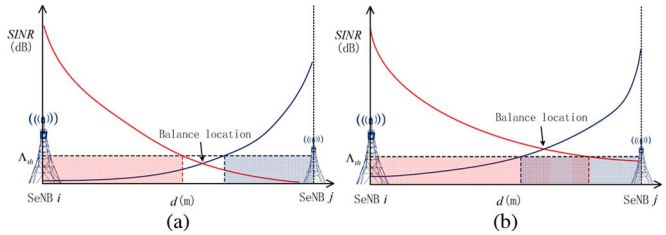

Fig. 2. Criterion of neighboring relationships. (a) Cells i and j are neighbors. (b) Cells i and j are not neighbors.

We define a matrix $\mathbf{\Lambda}$ to describe the neighboring relationships of small cells in the whole network. The element of matrix $\mathbf{\Lambda}$ can be defined as

$$\Lambda(i,j) = \begin{cases} 1, & \text{if } \widehat{\gamma}_{s,i}(x^*,y^*) > \Lambda_{\mathrm{th}} \\ 0, & \text{otherwise} \end{cases} \tag{7}$$

where $\Lambda(i,j) = 1$ means cells i and j are neighbors, whereas $\Lambda(i,j) = 0$ implies otherwise. Λ_{th} is a threshold variable that can be adjusted. When the SINR at the intersection of the curves exceeds Λ_{th}, the two small cells are considered neighbors. Fig. 3 illustrates the cell clustering results with different Λ_{th} for the same randomly generated scenario. The small cells that have overlaps belong to the same cell cluster. The red curves represent the coverage areas of cells in cochannel deployments, whereas the blue curves indicate the coverage areas of cells in orthogonal deployments. From Fig. 3, we can see that the size of a cell cluster expands when Λ_{th} decreases, and some nearby cell clusters might merge into new cell clusters. Consequently, the number of the cell clusters varies for different Λ_{th}. We can also notice that some small cells might stay out of any cluster even when Λ_{th} changes because they are isolated from other small cells. Since the deployment of the network is dynamic, the cell clustering result might change from slot to slot.

If a small cell is the neighbor of any small cell in a cell cluster, it is considered a member of that cell cluster. As a result, finding the cell clusters is equivalent to finding the connected subgraphs in a scattered graph. The algorithm for generating cell clusters is shown in Algorithm 1. In this algorithm, a is the index of a cell cluster, N_c is a variable that records the total number of cell clusters, and $\mathbf{C}$ is an array to hold all indices of the cell clusters.

Algorithm 1 Cell Clustering

Input: $\mathbf{S}$, $\mathbf{\Lambda}$.
Output: N_c, $\mathbf{C}$.
1: Initialization: $a := 1$, $N_c := 0$, $C(i) := 0$, $\forall\, i \in \mathbf{S}$.
2: **for** $\forall\, i,j \in \mathbf{S}$ *and* $i < j$ **do**
3: **if** *cell* i *and cell* j *are neighbors* **then**
4: **if** *Neither cell* i *nor cell* j *has been assigned to any cluster* **then**
5: Assign cell i and cell j to a new cluster a, $C(i) := C(j) := a$.
6: $a := a + 1$, $N_c := N_c + 1$.

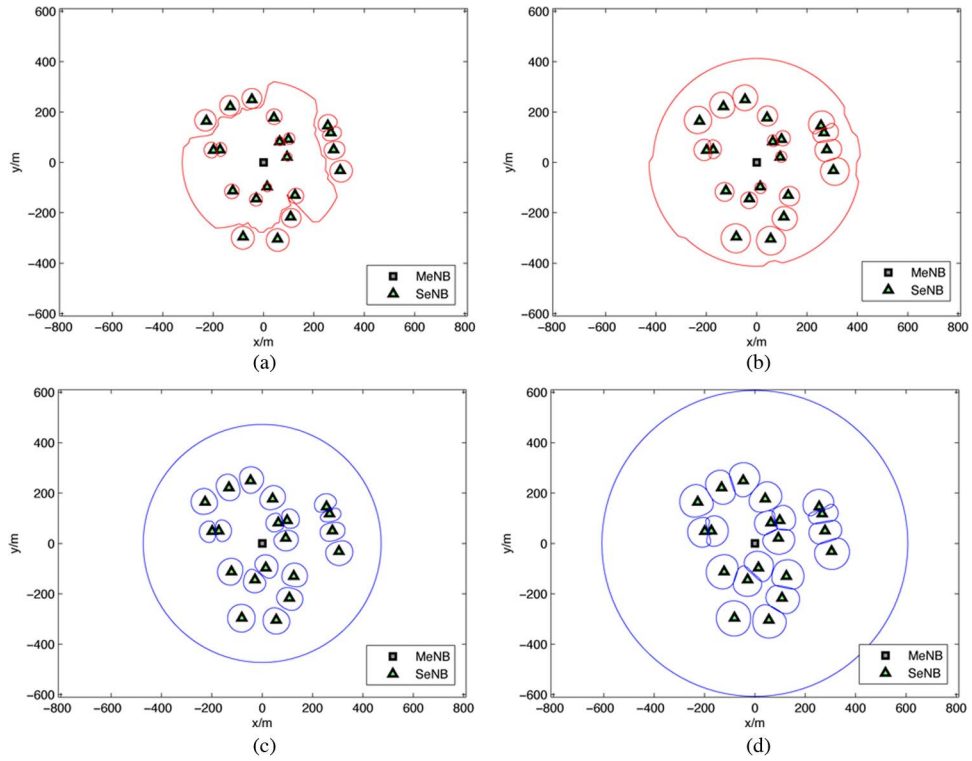

Fig. 3. Example of cell clustering with different $\Lambda_{\rm th}$ under different deployments. (a) $\Lambda_{\rm th} = 0$ dB, cochannel deployment. (b) $\Lambda_{\rm th} = -4$ dB, cochannel deployment. (c) $\Lambda_{\rm th} = 0$ dB, orthogonal deployment. (d) $\Lambda_{\rm th} = -4$ dB, orthogonal deployment.

TABLE II
RELATIVE INTERFERENCE FOR DIFFERENT UES

Co-channel Deployment	Orthogonal Deployment
$\rho_{m,k} = \frac{\sum_{i\in \mathbf{S}_k} P_{s,i} Loss_{s,i,k}}{P_m Loss_{m,k}}$	$\rho_{m,k} = 0$
$\rho_{s,i,k} = \frac{P_m Loss_{m,k} + \sum_{j\in \mathbf{S}_k, j\neq i} P_{s,j} Loss_{s,j,k}}{P_{s,i} Loss_{s,i,k}}$	$\rho_{s,i,k} = \frac{\sum_{j\in \mathbf{S}_k, j\neq i} P_{s,j} Loss_{s,j,k}}{P_{s,i} Loss_{s,i,k}}$

else if *Between cell i and cell j, one has been assigned to a cluster, say a'* **then**
  Assign cell i, cell j and their cluster members (if any) to the same cluster a'.
else
  $a' := \min(C(i), C(j))$.
  Assign cell i or cell j and its cluster members (if any) to the same cluster a'.
  $N_c := N_c - 1$.
end if
end if
end for

B. UE Clustering

We consider the UEs in an arbitrary cell cluster as vertices of a new subgraph with vertex set $\mathbf{V}$ and edge set $\mathbf{E}$. Each element of $\mathbf{E}$ corresponds to the interference relationship between the respective UEs. We use a metric named relative interference to describe the total interference impact of a MUE or SUE, which is defined as the ratio of the received interference power and signal power in the cell cluster. The metrics are denoted by $\rho_{m,k}$ and $\rho_{s,i,k}$ for MUEs and SUEs, respectively. We calculate the metric using the model of homogeneous Poisson point process [26]. Based on this model, we give the definition of relative interference for different UEs as listed in Table II, in which $\text{Loss}_{m,k}$ indicates the path loss between MeNB and UE k, and $\text{Loss}_{s,i,k}$ represents the path loss between SeNB i and UE k.

We define $\boldsymbol{S}_k$ as the set of cells in the cell cluster that contains UE k. For cochannel deployments, we simply take the macrocell as a member of the cell cluster that owns the maximum number of small cells so that the macrocell can achieve better coordination of interference with respect to other cell clusters. We can also use other methods, e.g., putting the macrocell in the cell cluster that is the closest one to the MeNB. When $\Lambda_{\rm th}$ is small enough to include all small cells in a cell cluster, cross-tier interference coordination occurs between the macrocell and all small cells. However, in orthogonal deployments, without cross-tier interference, we only need to consider the coordination among small cells.

The next task is to compute the weights of all the edges in each subgraph of the network. The weight of an edge represents the total relative interference at the two UEs k_1, k_2

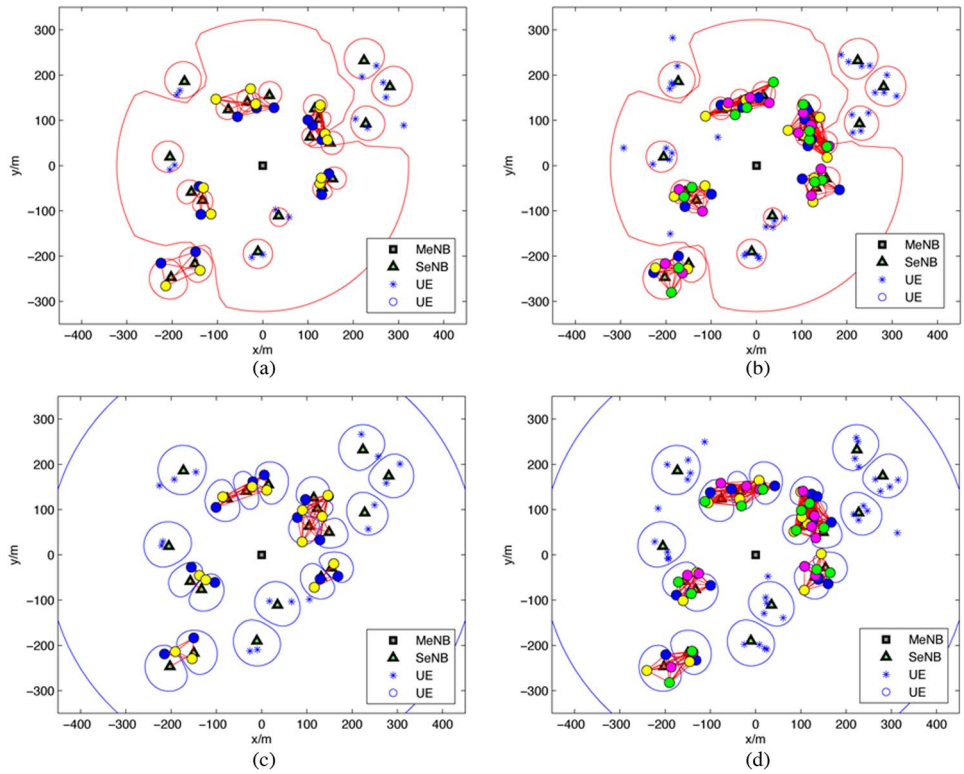

Fig. 4. UE clustering with a different number of UEs in different frequency deployments $\Lambda_{\rm th} = 0$ dB. (a) Number of UEs per cell is 2, cochannel deployment. (b) Number of UEs per cell is 4, cochannel deployment. (c) Number of UEs per cell is 2, orthogonal deployment. (d) Number of UEs per cell is 4, orthogonal deployment.

corresponding to the vertices connected by the edge, which is defined as

$$E(k_1,k_2) = E(k_2,k_1) = \begin{cases} \rho_{k_1} + \rho_{k_2}, & \text{if } k_1 \text{ and } k_2 \text{ are in different cells} \\ \rho_{k_1} + \rho_{k_2} + E_{\rm th}, & \text{otherwise} \end{cases} \quad (8)$$

where ρ_{k_1} and ρ_{k_2} represent the relative interference at UEs k_1 and k_2, respectively, and $E_{\rm th}$ is the upper bound of the weights in a UE cluster, which is set to limit the number of vertices in each UE cluster. In theory, $E_{\rm th}$ is equal to infinity. However, in practice, we set it to be a large enough value empirically considering the accuracy of the computing system. From the calculation method of $\mathbf{E}$, it is obvious that any two vertices from the same cell would not be assigned to the same UE cluster. The reason is, when any two vertices from the same cell are allocated to a UE cluster, the sum weight of that UE cluster would definitely be larger than $E_{\rm th}$. Therefore, to grow a UE cluster, it can only choose one vertex from each cell and continues to search for vertices from other cells.

We develop a subgraph clustering scheme to group vertices of every subgraph into UE clusters with minimum intracluster interference. The objective is to minimize the sum weight of all UE clusters. In this way if we assign the same subchannels to the UEs in the same UE cluster, the total interference is expected to be mitigated. The UE clustering process starts from a vertex randomly chosen from the subgraph. Iteratively, we traverse the subgraph by adding a vertex from other cells that minimizes the weight of the current UE cluster. When the sum weight of all vertices of a UE cluster reaches the upper bound $E_{\rm th}$, the UE cluster becomes isolated, and a new UE cluster starts to generate from the remaining vertices. Fig. 4 shows the UE clustering outcome for different number of UEs per cell. The UEs in each UE cluster are considered the vertices of the subgraph and the vertices with the same color belong to the same UE cluster in the subgraph.

The process of UE clustering is described in Algorithm 2. $\mathbf{V}$ is the set of vertices that have not been assigned. At the beginning, it holds all the vertices of the subgraph. The current candidate UE cluster is represented by $\boldsymbol{\zeta}$, and $\boldsymbol{\xi}$ is the candidate list that contains all candidate vertices to build the current UE cluster. We define the generated UE cluster set as $\boldsymbol{\Phi}$, and each element in $\boldsymbol{\Phi}$ indicates a UE cluster in the subgraph.

Algorithm 2 UE Clustering

Input: $\mathbf{V}$, $\mathbf{E}$.
Output: $\boldsymbol{\Phi}$.
1: Initialization: $\boldsymbol{\zeta}$ is empty, $\mathbf{V}$ contains all the vertices of the subgraph.
2: **while** $\mathbf{V}$ *is not empty* **do**
3: Randomly choose a vertex v from set $\mathbf{V}$, $\boldsymbol{\zeta} := \{v\}$.
4: Create a candidate list, $\boldsymbol{\xi} := \mathbf{V} \setminus \boldsymbol{\zeta}$.
5: **while** *sum weight of* $\boldsymbol{\zeta}$ *is less that* $E_{\rm th}$ **do**
6: Find the vertex v' from the candidate list $\boldsymbol{\xi}$ that minimizes the intrapath sum weight of the UE cluster.

Candidate cluster, $\boldsymbol{\zeta} := \boldsymbol{\zeta} \cup \{v'\}$.
end while
Remove the last vertex v', $\boldsymbol{\zeta} := \boldsymbol{\zeta} \setminus \{v'\}$.
Remove all the vertices of $\boldsymbol{\zeta}$ from set $\mathbf{V}$, $\mathbf{V} := \mathbf{V} \setminus \boldsymbol{\zeta}$, extract the vertices of $\boldsymbol{\zeta}$ as a new UE cluster and save it in $\boldsymbol{\Phi}$.
Reset $\boldsymbol{\zeta}, \boldsymbol{\xi} := \{\}$.
end while

C. Subchannel and Power Allocation

The joint subchannel and power allocation is an NP-hard problem that has exponential computational complexity [3]. We adopt a two-step scheme to separate subchannel allocation and power allocation [27], [28], which has been proved to be effective to reduce complexity while maintaining performance in OFDM-based systems. In Algorithm 3, we present a proportional fair scheduling scheme that iteratively assigns subchannels to UE clusters, which achieves maximum average UE throughput. The set of candidate subchannels for small cells is $\mathbf{N}_s$. In cochannel deployments, we have $\mathbf{N}_s = \mathbf{N}_m = \mathbf{N}$. The outcome of subchannel allocation is represented by set $\boldsymbol{\Psi}$ with dimension $1 \times N_s$, where subchannel n is assigned to the UE cluster with index $\Psi(n)$. Q_{cu} denotes the number of UE clusters in the cell cluster and the subchannels are assigned in $\lceil N_s/Q_{\mathrm{cu}} \rceil$ rounds.

Algorithm 3 Subchannel Allocation

Input: $\boldsymbol{\Phi}$, $\mathbf{N}_s$, Q_{cu}.
Output: $\boldsymbol{\Psi}$.
Initialization: $round := 1$.
while $\mathbf{N}_s$ *is not empty* **do**
  while $round <= \lceil N_s/Q_{\mathrm{cu}} \rceil$ **do**
    while $\boldsymbol{\Phi}$ *is not empty* **do**
      Let the selected UE cluster be $\boldsymbol{\phi}$, calculate the average UE throughput of $\boldsymbol{\phi}$ for each subchannel and find the best subchannel n^*.
      Save the index of UE cluster $\boldsymbol{\phi}$ to the n^*th element of $\boldsymbol{\Psi}$ and exclude $\boldsymbol{\phi}$ from $\boldsymbol{\Phi}$, $\boldsymbol{\Phi} := \boldsymbol{\Phi} \setminus \{\boldsymbol{\phi}\}$.
      Exclude subchannel n^* from the subchannel set $\mathbf{N}_s := \mathbf{N}_s \setminus \{n^*\}$.
    end while
  end while
  Reset $\boldsymbol{\Phi}$.
  $round := round + 1$.
end while

Once we assign all subchannels among all UE clusters, we use the water-filling method [4] to optimize power allocation among all assigned subchannels in each cell. We finally calculate the capacity of the whole network based on the results of subchannel and power allocations. For the cells that have not been assigned to any cell cluster, we conduct the same subchannel and power allocation scheme in those cells separately.

D. Computational Complexity

Given that the number of small cells is S, the complexity of cell clustering can be calculated as $((S-1)+(S-2)+\cdots+1)$, which is $O(S^2)$. We define the number of the generated cell clusters as N_c, the average number of small cells in each cell cluster as $\bar{N}_{cs}$, and $\bar{M}_s$ as the average number of UEs in each small cell. Then the complexity of UE clustering is $(N_c(\bar{N}_{cs}-1)[\bar{M}_s+(\bar{M}_s-1)+\cdots+1])$. Simplifying the expression and considering the worst case, the complexity results in $O(S^2M^2)$. For subchannel allocation, each UE cluster from the sorted list takes the best subchannel from the remaining subchannels; therefore, the complexity for one UE cluster is $(N_s+(N_s-1)+\cdots+1)$. Therefore, the complexity of subchannel allocation algorithm is $O(SN^2)$. Finally, for power allocation using water filling, the complexity is $O(SN)$. As a result, the total complexity of the graph-based approach is $O(S^2M^2+SN^2)$.

V. Dual-Based Approach

We present a dual-based approach for orthogonal deployments, which can be easily extended for cochannel deployments. This part is dedicated to solving problem (2), which is a nonconvex and NP-hard optimization problem. We can relax the region of $\boldsymbol{x}_s$ from $\{0, 1\}$ to [0, 1] in C9; then, problem (2) turns into a convex problem [29], in which the objective function is concave, and the constraints are all convex. According to [25], the duality gap of problem (2) is zero when the number of subchannels goes to infinity, which means that we can obtain the optimal solution from the dual problem instead of the primal one. Furthermore, the optimal solution can be obtained by solving the Karush–Kuhn–Tucker (KKT) conditions [30].

The Lagrangian function based on (2) can be expressed by

$$\begin{aligned} L(\boldsymbol{p}_s, \boldsymbol{x}_s, \boldsymbol{\alpha}, \boldsymbol{\beta}) = & \sum_{i\in\mathbf{S}} \sum_{k\in\mathbf{M}_{s,i}} w_{s,i,k} \sum_{n\in\mathbf{N}_s} x_{s,i,k,n} R_{s,i,k,n} \\ & + \sum_{i\in\mathbf{S}} \sum_{n\in\mathbf{N}_s} \beta_{i,n} \left(1 - \sum_{k\in\mathbf{M}_{s,i}} x_{s,i,k,n}\right) \\ & + \sum_{i\in\mathbf{S}} \alpha_i \left(P_{s,i} - \sum_{k\in\mathbf{M}_{s,i}} \sum_{n\in\mathbf{N}_s} p_{s,i,k,n}\right) \end{aligned} \tag{9}$$

where α_i and $\beta_{i,n}$ are the Lagrange multipliers, and $\boldsymbol{p}_s, \boldsymbol{x}_s, \boldsymbol{\alpha}$, and $\boldsymbol{\beta}$ are the matrices that hold $p_{s,i,k,n}, x_{s,i,k,n}, \alpha_i$ and $\beta_{i,n}$, respectively. We differentiate the Lagrangian over each $p_{s,i,k,n}$; thus, we have

$$\frac{\partial L}{\partial p_{s,i,k,n}} = \sum_{i\in\mathbf{S}} w_{s,j,k} x_{s,j,k,n} \frac{\partial R_{s,j,k,n}}{\partial p_{s,i,k,n}} - \alpha_i \quad \forall\, i \in \mathbf{S}, k \in \mathbf{M}_{s,i}, n \in \mathbf{N}_s. \tag{10}$$

To obtain the optimal $\boldsymbol{p}_s$, we first optimize $\boldsymbol{p}_s$ given $\boldsymbol{x}_s$ and $\boldsymbol{\alpha}$. Let the differentiation (10) equal to 0; we can get a set of (11), shown at the bottom of the next page, with variable $\boldsymbol{p}_s$.

TABLE III
SIMULATION PARAMETERS

Parameter	Value
Carrier Frequency	2 GHz
Total Bandwidth	12 MHz
Bandwidth per subchannel	180 KHz
Number of subchannels	64
Number of Small Cells	$4, 8, 12, 16, 20, 24, 28, 32$
Number of UEs per Cell	16
Path Loss Model for Macro Cell	$128.1 + 37.6\log_{10}(R)$ dB, R in km
Path Loss Model for Small Cell	$140.7 + 37.6\log_{10}(R)$ dB, R in km
Traffic Model for UEs	Best Effort Traffic
Maximum Tx Power of MeNB	46 dBm
Maximum Tx Power of SeNB	$28, 30, 32, 34, 36, 38$ dBm
Typical Cell Radius of Macro Cell	289 m
Typical Cell Radius of Small Cell	40 m
Bit Error Rate(BER)	10^{-3}
Thermal Noise	-174 dBm/Hz

Both (11) and the boundary constraint C12 in problem (2) are part of the KKT conditions [30]. Due to the zero duality gap between the primal and dual problems we claimed before, we can obtain the closed-form power allocation for all the eNBs by solving the KKT conditions. It is obvious that the number of equations and variables in (11) are equal; thus, we can easily solve the equations by transforming them into a least squares problem [31]. The least squares problem can be solved in a few iterations, and let the results be denoted by

$$p^*_{s,i,k,n} = x_{s,i,k,n} h_{s,i,k,n}(\boldsymbol{x}_s, \boldsymbol{\alpha}) \qquad \forall i \in \mathbf{S}, k \in \mathbf{M}_{s,i}, n \in \mathbf{N}_s \tag{12}$$

where $h_{s,i,k,n}$ is a function of $\boldsymbol{x}_s$ and $\boldsymbol{\alpha}$. In an OFDM-based system, the power allocation has strong connection to the subchannel allocation. Given $x_{s,i,k,n} = 1$, we have $p^*_{s,i,k,n} = h_{s,i,k,n}(\boldsymbol{x}_s, \boldsymbol{\alpha})$, while given $x_{s,i,k,n} = 0$, we have $p^*_{s,i,k,n} = 0$.

Substitution of $\boldsymbol{p}^*_s$ in the Lagrangian function $L(\boldsymbol{p}_s, \boldsymbol{x}_s, \boldsymbol{\alpha}, \boldsymbol{\beta})$ yields

$$L(\boldsymbol{p}^*_s, \boldsymbol{x}_s, \boldsymbol{\alpha}, \boldsymbol{\beta}) = \sum_{i \in \mathbf{S}} \left[\sum_{k \in \mathbf{M}_{s,i}} \sum_{n \in \mathbf{N}_s} x_{s,i,k,n} \left(w_{s,i,k} R_{s,i,k,n} - \alpha_i p^*_{s,i,k,n} - \beta_{i,n} \right) + \alpha P_{s,i} + \sum_{n \in \mathbf{N}_s} \beta_{i,n} \right]. \tag{13}$$

Next, we optimize $L(\boldsymbol{p}^*_s, \boldsymbol{x}_s, \boldsymbol{\alpha}, \boldsymbol{\beta})$ over $\boldsymbol{x}_s$. Finally, the objective function of the dual problem can be expressed as

$$\begin{aligned} L(\boldsymbol{\alpha}, \boldsymbol{\beta}) &= \sup_{\boldsymbol{x}_s \in \mathcal{X}} L\left(\boldsymbol{p}^*_s, \boldsymbol{x}_s, \boldsymbol{\alpha}, \boldsymbol{\beta}\right) \\ &= \sum_{i \in \mathbf{S}} \left[\sum_{k \in \mathbf{M}_{s,i}} \sum_{n \in \mathbf{N}_s} \left(w_{s,i,k} R_{s,i,k,n} - \alpha_i p^*_{s,i,k,n} - \beta_{i,n} \right)^+ + \alpha_i P_{s,i} + \sum_{n \in \mathbf{N}_s} \beta_{i,n} \right] \end{aligned} \tag{14}$$

where $\mathcal{X}$ is the solution space of $\boldsymbol{x}_s$. Accordingly, the dual problem can be formulated as follows:

$$\begin{aligned} \min \quad & L(\boldsymbol{\alpha}, \boldsymbol{\beta}) \\ \text{s.t.} \quad & \boldsymbol{\alpha} \succeq 0, \boldsymbol{\beta} \succeq 0. \end{aligned} \tag{15}$$

As we mentioned earlier, the duality gap between the primal problem (2) and dual problem (15) can be ignored when the number of subchannels is large. Consequently, we can achieve an optimal solution $(\boldsymbol{p}^*_s, \boldsymbol{x}^*_s)$ by minimizing the dual problem over $\boldsymbol{\alpha}$ and $\boldsymbol{\beta}$.

For $\boldsymbol{\alpha} \succeq 0$, we have

$$L(\boldsymbol{\alpha}) = \min_{\boldsymbol{\beta} \succeq 0} g(\boldsymbol{\alpha}, \boldsymbol{\beta}) = \sum_{i \in \mathbf{S}} \alpha_i P_{s,i} + \sum_{i \in \mathbf{S}} \sum_{n \in \mathbf{N}_s} \beta^*_{i,n}. \tag{16}$$

$$- \sum_{j \in \mathbf{S}, j \neq i} \frac{w_{s,j,k} x_{s,j,k,n} p_{s,j,k,n} g_{s,j,k,n} g_{s,i,k,n}}{\left(\sum_{c \in \mathbf{S}, c \neq j} \sum_{q \in \mathbf{M}_{s,c}} p_{s,c,q,n} g_{s,c,k,n} + \delta^2 \right)^2 + \Gamma p_{s,j,k,n} g_{s,j,k,n} \left(\sum_{c \in \mathbf{S}, c \neq j} \sum_{q \in \mathbf{M}_{s,c}} p_{s,c,q,n} g_{s,c,k,n} + \delta^2 \right)} + \frac{w_{s,i,k} x_{s,i,k,n} g_{s,i,k,n}}{\sum_{j \in \mathbf{S}, j \neq i} \sum_{q \in \mathbf{M}_{s,j}} p_{s,j,q,n} g_{s,j,k,n} + \delta^2} - \alpha_i \ln 2 = 0 \qquad \forall i \in \mathbf{S}, k \in \mathbf{M}_{s,i}, n \in \mathbf{N}_s \tag{11}$$

For any subchannel n in cell i, we can derive the minimum of $\beta^*_{i,n}$ according to

$$\beta^*_{i,n}(\boldsymbol{\alpha}) = \max_{k \in \mathbf{M}_{s,i}} w_{s,i,k} R_{s,i,k,n} - \alpha_i p^*_{s,i,k,n}. \quad (17)$$

Moreover, we can obtain the subchannel allocation decision in each cell i, e.g., subchannel n is assigned to UE $k^*(i,n)$, which is determined by

$$k^*(i,n) = \arg\max_{k \in \mathbf{M}_{s,i}} w_{s,i,k} R_{s,i,k,n} - \alpha_i p^*_{s,i,k,n} \quad \forall\, i \in \mathbf{S}, n \in \mathbf{N}_s. \quad (18)$$

Therefore, the subchannel allocation solution can be indicated as

$$x_{s,i,k,n} = \begin{cases} 1, & \text{if } k = k^*(i,n) \\ 0, & \text{else} \end{cases} \quad \forall\, i \in \mathbf{S}, n \in \mathbf{N}_s. \quad (19)$$

As the final step, the problem is solved by searching the minimum of $L(\boldsymbol{\alpha})$ in the feasible space region of $\boldsymbol{\alpha}$. We adopt subgradient search to find the solution, and give the parameter updating rule as follows:

$$\alpha_i^{z+1} = \left[\alpha_i^z - \tau_i^z \left(P_{s,i} - \sum_{k \in \mathbf{M}_{s,i}} \sum_{n \in \mathbf{N}_s} p^z_{s,i,k,n} \right) \right]^+ \quad \forall\, i \in \mathbf{S} \quad (20)$$

where z is the iteration index, and τ_i^z is the step size of each iteration.

A. Computational Complexity

For the dual-based approach, the complexity can be calculated as $(I_1 I_2 S N_s \bar{M}_s)$, where I_1 is the number of iterations to solve the least squares problem, and I_2 is the number of iterations in the subgradient search. In the worst case, the computational complexity is $O(I_1^{\max} I_2^{\max} SNM)$, where $I_1^{\max}$ and $I_2^{\max}$ are, respectively, the maximum values of I_1 and I_2, which are obtained from Monte Carlo simulations.

VI. Simulation Results and Discussions

To validate the proposed graph-based approach, we present numerical examples and simulation results here. In our simulation setup, small cells are uniformly deployed in the typical coverage area of a macrocell, as recommended by 3GPP [32] considering the maximum transmit power of the eNB. For example, if the maximum transmit power of the eNB is 46 dBm, the typical cell radius is 289 m. The values of parameters are chosen following the guidelines of 3GPP [32], and the primary system parameters are summarized in Table III. We consider Rayleigh fading to model the channels between eNBs and UEs. We take the results from Monte Carlo simulations with 10 000 trials. In each trial, we generate the locations of SeNBs and UEs randomly. We consider that the UEs move at a low speed ($<$ 3km/h), and the UEs are saturated with best-effort traffic [33].

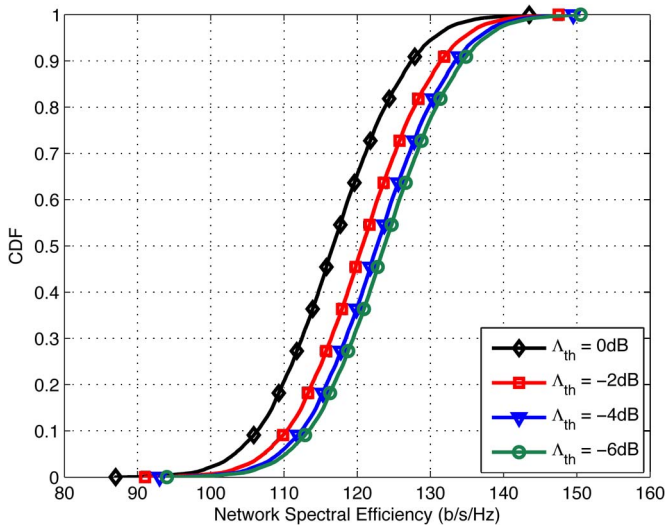

Fig. 5. CDF of network spectral efficiency under different $\Lambda_{\rm th}$, the number of small cells is 20, and the maximum transmit power of SeNB is 30 dBm.

A. Network Spectral Efficiency Under Different $\Lambda_{\rm th}$

Here, we examine the network performance under different $\Lambda_{\rm th}$. First, we evaluate the performance of the graph-based approach under cochannel deployments. Fig. 5 presents the cumulative distribution function (cdf) of the whole network's capacity. The results show that when $\Lambda_{\rm th}$ decreases, the cell clusters grow and the efficiency of the whole network increases. In other words, when $\Lambda_{\rm th}$ is decreased, there is more cooperation among the small cells so that the graph-based approach plays a more important role to coordinate interference, which results in better network efficiency. A similar trend is observed in the orthogonal deployments. These results show the efficacy of our interference coordination scheme.

B. Network Spectral Efficiency in Different Deployments

Next, we compare the network performance in two different deployments. In cochannel deployments, macrocell and small cells share all 64 subchannels, whereas in orthogonal deployments, we preassign a number of subchannels for MUEs and the remaining for SUEs. We simulate the scenarios when the macrocell owns 16, 24, 32, 40, and 48 subchannels and compare them with the scenario of cochannel deployments. The cdfs of network efficiency for these scenarios are presented in Fig. 6. The figure shows that cochannel deployments can achieve better network efficiency compared to orthogonal deployments in our system configuration. In orthogonal deployments, the network efficiency decreases with the increasing number of subchannels assigned to the macrocell. Furthermore, we compare the average UE spectral efficiency between the two deployments in Fig. 7. The figure shows that the average MUE spectral efficiency has positive correlations with the number of subchannels dedicated for it, whereas the SUEs react in the opposite manner. The increasing trend of average MUE spectral efficiency and the decreasing trend of that for SUE are quite close. However, due to the various numbers of UEs in the two types of cells, the whole network efficiency differs a lot between

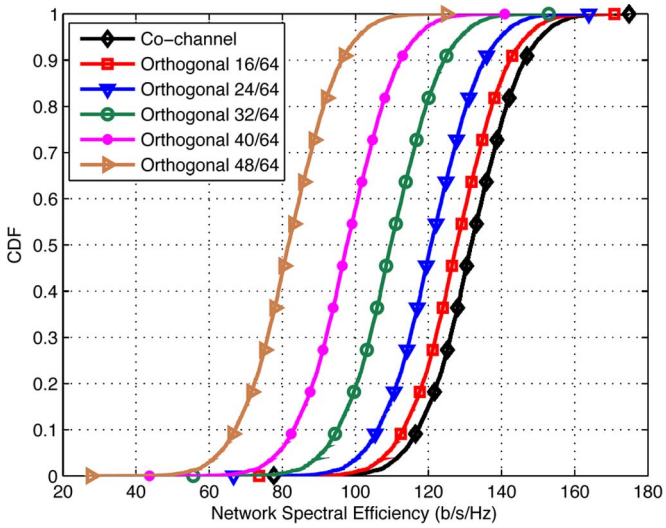

Fig. 6. CDF of network spectral efficiency under different deployments, $\Lambda_{\rm th} = 0$ dB, the number of small cells is 20, and the maximum transmit power of SeNB is 30 dBm.

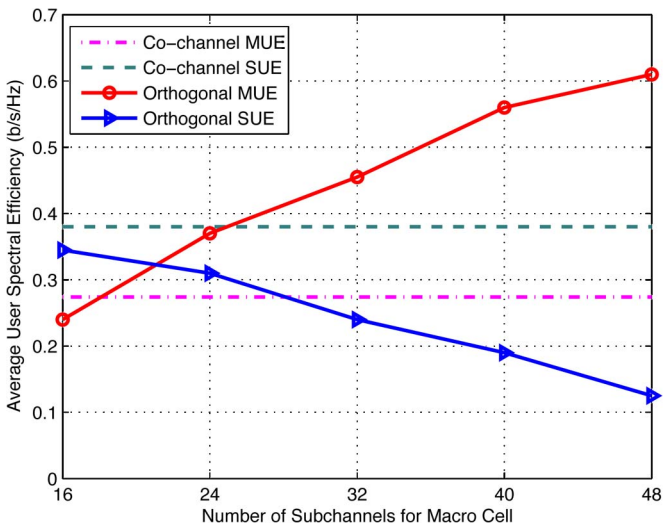

Fig. 7. Average UE spectral efficiency under different deployments, $\Lambda_{\rm th} = 0$ dB, the number of small cells is 20, and the maximum transmit power of SeNB is 30 dBm.

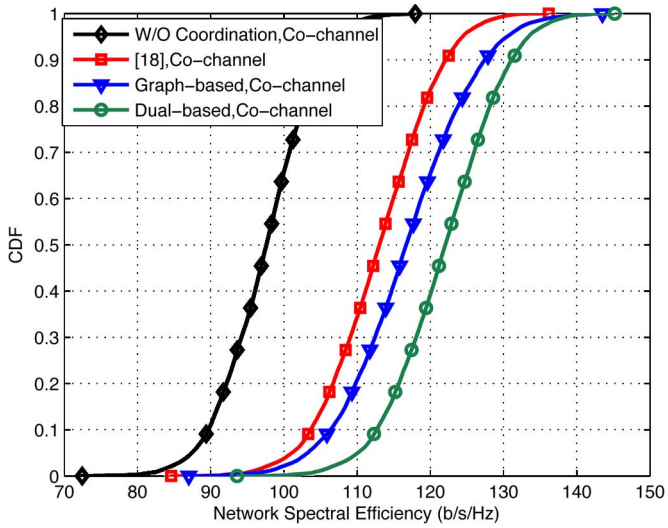

Fig. 8. CDF of network spectral efficiency under different schemes, $\Lambda_{\rm th} = 0$ dB, subchannels for macrocell is 16 in orthogonal deployments, the number of small cells is 20, and the maximum transmit power of SeNB is 30 dBm.

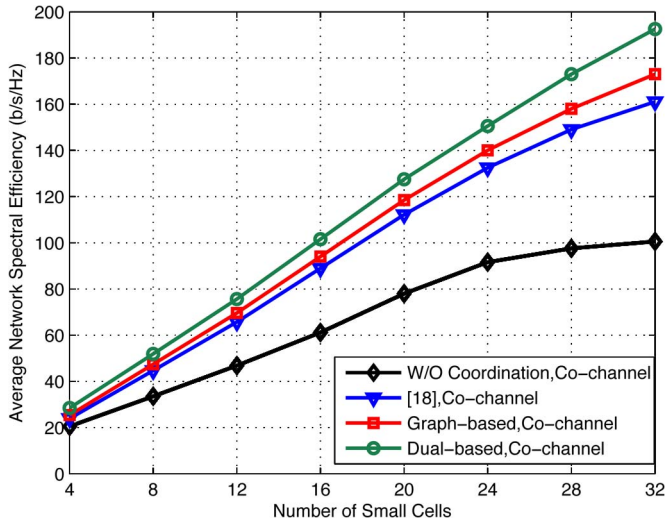

Fig. 9. Average network spectral efficiency versus small cell number under different schemes, $\Lambda_{\rm th} = 0$ dB, and the maximum transmit power of SeNB is 30 dBm.

the two deployments. We observe that the average SUE spectral efficiency under cochannel deployments achieves a better performance, even when only a small portion of subchannels are assigned to the macrocell.

C. Comparison With Other Approaches

Next, we compare our graph-based approach with the proposed dual-based approach, our former approach [18], and the distributed approach without interference coordination. In the distributed approach, we adopt the same subchannel and power allocation method as in the graph-based approach and implement it in each cell, which is equivalent to the extreme case that treats each cell as a cell cluster in the graph-based approach. In Fig. 8, we observe notable performance improvements of our three approaches compared with the distributed approach in cochannel deployments. It is obvious that the graph-based approach achieves far better performance as the distributed approach is completely ignorant of the cross-tier or the cotier interference. Moreover, our graph-based approach achieves better performance than our former approach [18]. Moreover, the graph-based approach can achieve more than 90% of the performance of the dual-based approach while incurring much lower computation complexity, which is more suitable for real-time implementation. We obtain a similar trend of performance improvement in our graph-based approach under orthogonal deployments. Fig. 9 compares the performance of the graph-based approach with the other three approaches in cochannel deployments when the number of small cells is increased. The same number of UEs is assumed in the added small cells. From the figure, with an increasing number of small cells, the spectrum efficiency of the three approaches increases linearly at first. However, when the deployment of small cells becomes

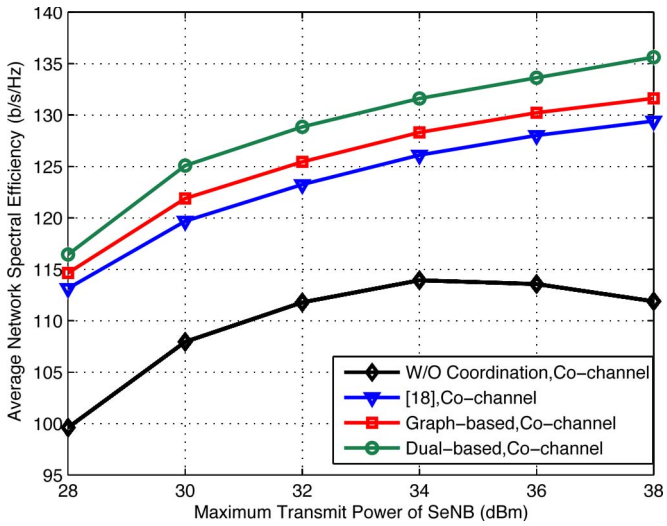

Fig. 10. Average network spectral efficiency versus maximum transmit power of SeNB under different schemes, $\Lambda_{\rm th} = 0$ dB, and the number of small cells is 20.

dense, the rates of increment decrease. We can observe that the growth of spectrum efficiency with the distributed approach decreases first, and the gap of the distributed approach and the graph-based approach increases as the number of small cells grows.

Finally, we compare the average network spectral efficiency of the graph-based approach with the other three approaches by varying the maximum power of SeNBs. In Fig. 10, we can see that as the transmit power of SeNB is increased from 28 to 38 dBm, the average network spectral efficiency increases for all the approaches, except that, beyond 34 dBm, the performance of the distributed approach starts decreasing as the network becomes interference limited. While the other approaches have much better performance than the distributed approach particularly at a high level of maximum SeNB power, the graph-based approach only slightly underperform the dual-based approach but outperform the approach in [18]. We also obtain similar results in orthogonal deployments.

VII. Conclusion

In this paper, we have presented a novel graph-based resource allocation approach for OFDM-based HCNs. In our approach, two types of clustering schemes, i.e., cell clustering and UE clustering, are involved to mitigate the downlink cross-tier and cotier interference. To show the efficacy and effectiveness of the proposed graph-based approach, we have introduced a dual-based approach to search for the optimal solution of the formulated problem. We have conducted extensive simulations and the results showed that significant improvement in spectral efficiency can be achieved comparing with the distributed approach without considering interference coordination both in cochannel and orthogonal deployments. Furthermore, the graph-based approach can obtain near-optimal performance with much lower computation complexity. In the future work, we will study the problem of uplink scheduling in HCNs, which is a more challenging work, particularly when we consider severe mutual interference in the dynamic system. Furthermore, the combination of downlink and uplink scheduling could be a good research item to further enhance system performance.

References

[1] Cisco Visual Networking Index: Global Mobile Data Trafc Forecast Update, 2013–2018, Cisco, San Jose, CA, USA, 2013. [Online]. Available: http://www.cisco.com

[2] A. Hamza, S. Khalifa, H. Hamza, and K. Elsayed, "A survey on inter-cell interference coordination techniques in OFDMA-based cellular networks," *IEEE Commun. Surveys Tuts.*, vol. 15, no. 4, pp. 1642–1670, 4th Quart. 2013.

[3] Z.-Q. Luo and S. Zhang, "Dynamic spectrum management: Complexity and duality," *IEEE J. Sel. Topics Signal Process.*, vol. 2, no. 1, pp. 57–73, Feb. 2008.

[4] D. P. Palomar and J. R. Fonollosa, "Practical algorithms for a family of water-filling solutions," *IEEE Trans. Signal Process.*, vol. 53, no. 2, pp. 686–695, Feb. 2005.

[5] N. Saquib, E. Hossain, L. B. Le, and D. I. Kim, "Interference management in ofdma femtocell networks: Issues and approaches," *IEEE Wireless Commun.*, vol. 19, no. 3, pp. 86–95, Jun. 2012.

[6] K. I. Pedersen, Y. Wang, S. Strzyz, and F. Frederiksen, "Enhanced inter-cell interference coordination in co-channel multi-layer LTE-advanced networks," *IEEE Wireless Commun.*, vol. 20, no. 3, pp. 120–127, Jun. 2013.

[7] C. Kosta, B. Hunt, A. Quddus, and R. Tafazolli, "On interference avoidance through inter-cell interference coordination (ICIC) based on OFDMA mobile systems," *IEEE Commun. Surveys Tuts.*, vol. 15, no. 3, pp. 973–995, 3rd Quart. 2013.

[8] Y. Wang, Y. Chang, and D. Yang, "An efficient inter-cell interference coordination scheme in heterogeneous cellular networks," in *Proc. IEEE VTC Fall*, 2012, pp. 1–5.

[9] H. Marshoud, H. Otrok, H. Barada, R. Estrada, and Z. Dziong, "Genetic algorithm based resource allocation and interference mitigation for OFDMA macrocell-femtocells networks," in *Proc. 6th Joint IFIP WMNC*, 2013, pp. 1–7.

[10] D. Ling, Z. Lu, Y. Ju, X. Wen, and W. Zheng, "A multi-cell adaptive resource allocation scheme based on potential game for ICIC in LTE-A," *Int. J. Commun. Syst.*, vol. 27, no. 11, pp. 2744–2761, Nov. 2014.

[11] Z. Lu, Y. Yang, X. Wen, Y. Ju, and W. Zheng, "A cross-layer resource allocation scheme for ICIC in LTE-advanced," *J. Netw. Comput. Appl.*, vol. 34, no. 6, pp. 1861–1868, Nov. 2011.

[12] R. Xie, F. Yu, H. Ji, and Y. Li, "Energy-efficient resource allocation for heterogeneous cognitive radio networks with femtocells," *IEEE Trans. Wireless Commun.*, vol. 11, no. 11, pp. 3910–3920, Nov. 2012.

[13] S. Sadr and R. Adve, "Hierarchical resource allocation in femtocell networks using graph algorithms," in *Proc. IEEE ICC*, 2012, pp. 4416–4420.

[14] E. Pateromichelakis, M. Shariat, R. Tafazolli, and A. ul Quddus, "On the evolution of multi-cell scheduling in 3GPP LTE/LTE-A," *IEEE Commun. Surveys Tuts.*, vol. 15, no. 2, pp. 701–717, 2nd Quart. 2013.

[15] M. C. Necker, "Scheduling constraints and interference graph properties for graph-based interference coordination in cellular OFDMA networks," *Mobile Netw. Appl.*, vol. 14, no. 4, pp. 539–550, Aug. 2009.

[16] R. Y. Chang, Z. Tao, J. Zhang, and C.-C. Kuo, "Multicell OFDMA downlink resource allocation using a graphic framework," *IEEE Trans. Veh. Technol.*, vol. 58, no. 7, pp. 3494–3507, Sep. 2009.

[17] H. Li *et al.*, "Graph method based clustering strategy for femtocell interference management and spectrum efficiency improvement," in *Proc. 6th Int. Conf. WiCOM Netwo. Mobile Comput.*, 2010, pp. 1–5.

[18] L. Zhou *et al.*, "A graph-based resource allocation scheme with interference coordination in small cell networks," in *Proc. IEEE GLOBECOM Workshop*, 2014, pp. 1223–1228.

[19] S.-H. Park, O. Simeone, O. Sahin, and S. Shamai, "Joint base station selection and distributed compression for cloud radio access networks," in *Proc. IEEE GLOBECOM Workshops*, 2012, pp. 1134–1138.

[20] S. Sun and Y. Jing, "Channel training design in amplify-and-forward mimo relay networks," *IEEE Trans. Wireless Commun.*, vol. 10, no. 10, pp. 3380–3391, Oct. 2011.

[21] S. Sun and Y. Jing, "Training and decodings for cooperative network with multiple relays and receive antennas," *IEEE Trans. Commun.*, vol. 60, no. 6, pp. 1534–1544, Jun. 2012.

[22] Z. Shen, J. G. Andrews, and B. L. Evans, "Short range wireless channel prediction using local information," in *Proc. IEEE ACSSC*, 2003, vol. 1. pp. 1147–1151.

[23] I. C. Wong, A. Forenza, R. W. Heath, and B. L. Evans, "Long range channel prediction for adaptive OFDM systems," in *Proc. IEEE ACSSC*, 2004, vol. 1. pp. 732–736.
[24] C.-H. Fung, W. Yu, and T. J. Lim, "Precoding for the multiantenna downlink: Multiuser SNR gap and optimal user ordering," *IEEE Trans. Commun.*, vol. 55, no. 1, pp. 188–197, Jan. 2007.
[25] W. Yu and R. Lui, "Dual methods for nonconvex spectrum optimization of multicarrier systems," *IEEE Trans. Commun.*, vol. 54, no. 7, pp. 1310–1322, Jul. 2006.
[26] H. P. Keeler, B. Blaszczyszyn, and M. K. Karray, "SINR-based k-coverage probability in cellular networks with arbitrary shadowing," in *Proc. IEEE ISIT*, 2013, pp. 1167–1171.
[27] J. Jang and K. B. Lee, "Transmit power adaptation for multiuser OFDM systems," *IEEE J. Sel. Areas Commun.*, vol. 21, no. 2, pp. 171–178, Feb. 2003.
[28] Z. Shen, J. G. Andrews, and B. L. Evans, "Adaptive resource allocation in multiuser OFDM systems with proportional rate constraints," *IEEE Trans. Wireless Commun.*, vol. 4, no. 6, pp. 2726–2737, Nov. 2005.
[29] J. Huang, V. G. Subramanian, R. Agrawal, and R. A. Berry, "Downlink scheduling and resource allocation for OFDM systems," *IEEE Trans. Wireless Commun.*, vol. 8, no. 1, pp. 288–296, Jan. 2009.
[30] S. Boyd and L. Vandenberghe, *Convex Optimization*. Cambridge, U.K.: Cambridge Univ. Press, 2009.
[31] J. Nocedal and S. J. Wright, *Least-Squares Problems*. Berlin, Germany: Springer-Verlag, 2006.
[32] Third-Generation Partnership Project (3GPP), "Evolved universal terrestrial radio access (E-UTRA): Radio frequency(RF) system scenarios," Sophia Antipolis, France, TR 36.942 V11.0.0, 2012. [Online]. Available: http://www.3gpp.org/ftp/specs
[33] Z. Jiang, Y. Ge, and Y. Li, "Max-utility wireless resource management for best-effort traffic," *IEEE Trans. Wireless Commun.*, vol. 4, no. 1, pp. 100–111, Jan. 2005.

Li Zhou received the B.S. and M.S. degrees from the National University of Defense Technology (NUDT), Changsha, China, in 2009 and 2011, respectively. He is currently working toward the Ph.D. degree with the College of Electronic Science and Engineering, NUDT.

From September 2013 to September 2014, he was a Visiting Scholar with The University of British Columbia, Vancouver, BC, Canada. His research interests include cell planning, scheduling, and resource allocation in heterogeneous cellular networks.

Xiping Hu is currently working toward the Ph.D. degree with the Department of Electrical and Computer Engineering, The University of British Columbia (UBC), Vancouver, BC, Canada.

He is the Cofounder and Chief Technology Officer of Bravolol, Hong Kong: a leading language learning mobile application company with over 40 million accumulate downloads and 6 million monthly active users. He is the author or coauthor of papers presented and published in 20 prestigious international conferences and journals, such as the IEEE Hawaii International Conference on System Sciences; the IEEE TRANSACTIONS ON EMERGING TOPICS IN COMPUTING; IEEE COMMUNICATIONS MAGAZINE, IEEE COMMUNICATIONS SURVEYS & TUTORIALS; the ACM International Conference on Mobile Systems, Applications, and Services; the ACM Conference on Embedded Networked Sensor Systems; and the ACM Annual International Conference on Mobile Computing and Networking. He is a Microsoft Certified Specialist in web applications, .NET Framework, and SQL server. He was a key member in several research projects, such as the web service security identification project at Tsinghua University, Beijing, China, the SAVOIR project at the National Research Council of Canada–Institute for Information Technology (NRC–IIT), and the NSERC DIVA strategy research network at UBC.

Mr. Hu has received the Silver Prizes in national Olympic competitions in mathematics and physics in China. His research interests include mobile social networks, mobile computing, and crowdsourced sensing.

Edith C.-H. Ngai (M'07) received the Ph.D. degree from The Chinese University of Hong Kong, Hong Kong, in 2007.

From 2007 to 2008, she was a Postdoctoral Researcher with Imperial College London, London, U.K. She has also conducted research with Simon Fraser University, Burnaby, BC, Canada; Tsinghua University, Beijing, China; and the University of California, Los Angeles, CA, USA. She is currently an Associate Professor with the Department of Information Technology, Uppsala University, Uppsala, Sweden. Her research interests include wireless sensor and mobile networks, Internet of Things, network security and privacy, smart cities, and e-health applications.

Dr. Ngai has served as a Technical Program Committee (TPC) member for the IEEE International Conference on Distributed Computing Systems, the IEEE Conference on Computer Communications, the IEEE International Conference on Communications, the IEEE Global Communications Conference, the IEEE/ACM International Workshop on Quality of Service, the IEEE International Conference on Distributed Computing in Sensor Systems, the IEEE Conference on Local Computer Networks, etc. She served as a TPC Cochair for the 2012 Swedish National Computer Networking Workshop and the Tenth International Conference on Heterogeneous Networking for Quality, Reliability, Security, and Robustness. She serves as a Program Cochair for ACM womENcourage 2015 and the TPC Cochair for SmartCity 2015 and the 2015 Tenth International Conference on Intelligent Sensors, Sensor Networks, and Information Processing. She has been a Guest Editor for special issues in THE IEEE INTERNET OF THINGS JOURNAL, *Springer MONET*, *and the EURASIP Journal on Wireless Communications and Networking*. She coreceived the Best Paper Runner-Up Awards at the IEEE International Workshop on Quality of Service in 2010 and at the International Conference on Information Processing in Sensor Networks in 2013. She has been a VINNMER Fellow of VINNOVA, Sweden, since 2009.

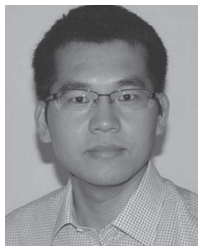

Haitao Zhao (M'14) received the B.S. and Ph.D. degrees in information and communication engineering from the National University of Defense Technology (NUDT), Changsha, China, in 2004 and 2009, respectively.

From April 2008 to July 2009, he was a Visiting Research Associate with the Institute of Electronics, Communications and Information Technology, Queen's University of Belfast, Belfast, U.K. He is currently an Associate Professor with the College of Electronic Science and Engineering, NUDT. He is the author of more than 50 research papers. His main research interests include cognitive radio networks, self-organized networks, and cooperative communications.

Dr. Zhao has served as a Technical Program Committee member of the Mobile and Wireless Networking Symposium of the 2014 IEEE International Conference on Communications. He is currently a mentor member of the IEEE 1900.1 standard and a member of World-wide University Network (WUN) Cognitive Communications Consortium. He has served as the Lead Guest Editor for the Special Issue *on Advances in Cognitive Radio Ad Hoc Networks (Hindawi Journal of Electrical and Computer Engineering)*.

Shan Wang received the B.S. and Ph.D. degrees from the National University of Defense Technology, Changsha, China, in 2000 and 2006, respectively.

From October 2010 to September 2011, he was a Visiting Researcher with the University of Montreal, Montreal, QC, Canada. He is currently an Associate Professor with the College of Electronic Science and Engineering, NUDT. His research interests include wireless protocol design and network simulation.

Jibo Wei received the B.S. and M.S. degrees from the National University of Defense Technology, Changsha, China, in 1989 and 1992, respectively, and the Ph.D. degree from Southeast University, Nanjing, China, in 1998, all in electronic engineering.

He is currently the Director and a Professor with the Department of Communication Engineering, NUDT. His research interests include wireless network protocols and signal processing in communications, particularly in the areas of multiple-input multiple-output, multicarrier transmission, cooperative communications, and cognitive networks.

Dr. Wei serves as an Editor for the *Journal on Communications*. He is a Senior Member of the China Institute of Communications and Electronics and a member of the IEEE Communication and Vehicular Technology Societies.

Victor C. M. Leung (S'75–M'89–SM'97–F'03) received the B.A.Sc. (Hons.) and Ph.D. degrees from The University of British Columbia, Vancouver, BC, Canada, in 1977 and 1981, respectively.

He is currently a Professor and a Holder of the TELUS Mobility Research Chair in Advanced Telecommunications Engineering with the Department of Electrical and Computer Engineering, The University of British Columbia. He has been involved in telecommunications research with a focus on wireless networks and mobile systems for more than 30 years, which has resulted in more than 700 journal and conference papers coauthored with his students and collaborators, including several papers that have won best paper awards.

Dr. Leung has contributed to the organization and technical program committees of numerous conferences. He was a Distinguished Lecturer of the IEEE Communications Society. He has contributed to the editorial boards of many journals, including the IEEE TRANSACTIONS ON COMPUTERS, the IEEE TRANSACTIONS ON WIRELESS COMMUNICATIONS, the IEEE TRANSACTIONS ON VEHICULAR TECHNOLOGY, IEEE WIRELESS COMMUNICATIONS LETTERS, and the IEEE JOURNAL ON SELECTED AREAS IN COMMUNICATIONS. He received an APEBC Gold Medal in 1977 as the head of the graduating class of the Faculty of Applied Science, a Natural Sciences and Engineering Research Council of Canada Postgraduate Scholarship during 1977–1981, an IEEE Vancouver Section Centennial Award in 2011, and a UBC Killam Research Prize in 2012. He is a Fellow of The Royal Society of Chemistry, the Engineering Institute of Canada, and The Canadian Academy of Engineering. He is a Registered Professional Engineer in the Province of British Columbia.